Influence of Ionization and Beam Quality on Interaction of TW-Peak CO2 Laser with Hydrogen Plasma

R. Samulyak,

Computational Science Initiative

Brookhaven National Laboratory

U.S. Department of Energy

USDOE Office of Science (SC), Advanced Scientific Computing Research (SC-21)

DISCLAIMER

INFLUENCE OF IONIZATION AND BEAM QUALITY ON INTERACTION OF TW-PEAK CO₂ LASER WITH HYDROGEN PLASMA

P. Kumar*, Stony Brook University, Stony Brook, NY 11794, USA

K. Yu [†], BNL, Upton, NY 11973, USA

R. Samulyak [‡], Stony Brook University, Stony Brook, NY 11794, and BNL, Upton, NY 11973, USA

Abstract

3D numerical simulations of the interaction of a powerful CO_2 laser with hydrogen jets demonstrating the role of ionization and laser beam quality are presented. Simulations are performed in support of the plasma wakefield accelerator experiments being conducted at the BNL Accelerator Test Facility (ATF). The CO_2 laser at BNL ATF has several potential advantages for laser wakefield acceleration compared to widely used solid-state lasers. SPACE, a parallel relativistic Particle-in-Cell code, developed at SBU and BNL, has been used in these studies. A novelty of the code is its set of efficient atomic physics algorithms that compute ionization and recombination rates on the grid and transfer them to particles. The primary goal of the initial BNL experiments was to characterize the plasma density by measuring the sidebands in the spectrum of the probe laser. Simulations, that resolve hydrogen ionization and laser spectra, help explain several trends that were observed in the experiments [1].

INTRODUCTION

Modern laser wake-field accelerators (LWFA) have achieved GeV-scale electron beams with very low transverse emittance [2]. But they have used inefficient solid-state laser drivers of petawatt peak power, producing small size plasma bubbles that are very chalenging for external electron injection, characterization and control, and suffered from large energy spreads and significant shot-to-shot instability, inhibiting FEL and HEP applications. CO_2 lasers are among the world's most efficient lasers, capable of producing large plasma bubbles, provide a promising alternative path to LWFA [3], [4]. Exploration of CO_2 laser power for LWFA is the main goal of the BNL ATF experimental program.

Highly resolved simulations of a spectrum of physics processes occurring during the interaction of a BNL-specs CO_2 laser with a hydrogen jet have been performed using a 3D parallel electromagnetic PIC code SPACE, developed at BNL and Stony Brook University [5]. SPACE is a general purpose PIC code and can be used in the study of a variety of beam-plasma and laser-plasma interaction problems. An important feature of the code is implementation of complex atomic physics processes. Simulations accurately resolve ionization processes in hydrogen gas and the formation of plasma, relativistic self-focusing of powerful laser beams, self-upshifting of the CO_2 laser frequency due to spatial

distributions of plasma density, and strong Stokes and anti-Stokes peaks in the electromagnetic spectrum caused by a nonlinear interaction with plasma wakes. In addition, the effect of laser beam quality parameter (M^2) on laser self-focusing, intensity of the Stoke/anti-Stokes side bands, and plasma wakes has been studied. The goal of these simulations is to guide future experiments at BNL ATF.

PROPAGATION OF CO₂ LASER IN H_2 GAS

When a $TW-$ peak power CO_2 laser with parameters presented in Table 1 propagates in a hydrogen jet, several important phenomena occur which influence the structure and characteristics of the plasma wakes produced.

Laser Self-modulation and Relativistic Self-focusing

Laser peak power $\left(P > P_c \approx 17 \left(\frac{\lambda_p}{\lambda} \right)^2 \right)$ and length of the pulse $\left(L = c\tau_L > \lambda_p \right)$ satisfy the conditions of self-modulated laser wakefield acceleration (SMLWFA) wherein a single laser pulse breaks up into smaller pulses via forward Raman scattering, producing periodic regions of focusing and diffraction [6]. This process is further enhanced by relativistic self-focusing which maintains the laser pulse at high normalized vector potential for several Rayleigh lengths [7]. The ponderomotive force of the laser expels electrons from the laser path and accelerates them to relativistic velocities leading to the relativistic mass increase. Combination of these two processes reduce the plasma frequency ω_p and increase the plasma refractive index η_R along the laser path relative to these quantities at the edge of the laser. In the presence of high-energy electromagnetic waves in plasma, η_R can be expressed as

$$\eta_R = \sqrt{1 - \frac{\omega_p^2}{\omega^2}}, \quad \text{where} \quad \omega_p = \sqrt{\frac{n_e e^2}{\gamma m_0 \epsilon_0}}. \quad (1)$$

Here n_e is a local electron number density and γm_0 is the electron relativistic mass. Along the laser path, the ponderomotive forces decrease n_e and increase γ. Since the phase velocity v_ϕ is c/η_R, a bigger refractive index in the center leads to self-focusing of the laser.

Table 1: Laser Parameters

Wavelength	Beam Waist	Duration	a_0
10.6 μm	20 μm	2 ps(FWHM)	2.9

---

* prabhat.kumar@stonybrook.edu

[†] kyu@bnl.gov

[‡] roman.samulyak@stonybrook.edu

03 Novel Particle Sources and Acceleration Technologies

A22 Plasma Wakefield Acceleration

Scattering of Laser with Electron Plasma Waves

When the electromagnetic radiation from the laser interacts with the electron plasma wave (EPW) created by the interaction of laser with hydrogen gas, it induces laser modulation that manifests itself as Stokes and anti-Stokes waves [6]. The frequency and wavenumber of these waves are given by $(\omega_0 - \omega_p, k_0 - k_p)$ and $(\omega_0 + \omega_p, k_0 + k_p)$ respectively, where (ω_0, k_0) is the frequency and wavenumber of the laser and (ω_p, k_p) is that of the plasma. In order to properly characterize the wakes generated by laser-plasma interaction, it is important to understand the relative width and spectral and spatial structure of these spectral side bands. The dependence of intensity of these side bands on the resolution of ionization processes and laser beam quality will be presented in the next section.

Ionization Model in SPACE

Accurate resolution of ionization processes is very important in simulations of the laser-matter interaction. Ionization effects such as creation of plasma through tunneling ionization, frequency up-shifting of the laser, harmonic generation and scattering instabilities play a major role in laser wakefield acceleration process [8]. A tunneling ionization algorithm has been implemented in code SPACE. A novelty of the code is its set of efficient atomic physics algorithms that compute ionization and recombination rates on the grid and transfer them to particles. Ionization probability rate, W (s^{-1}), depends only on local electric field (GV/m) and the ionization energy (eV) of neutral atoms as follows:

$$W(s^{-1}) \approx 1.52e^{15}\frac{4^{n^\star}\xi_i(eV)}{n^\star\Gamma(2n^\star)}\left(20.5\frac{\xi_i^{1.5}(eV)}{E(GV/m)}\right)$$
$$exp\left(-6.83\frac{\xi_i^{1.5}(eV)}{E(GV/m)}\right) \quad (2)$$

where $n^\star = 3.69Z/\sqrt{\xi_i eV}$ is the effective principal quantum number, Z being the atomic number of the neutral gas. Number of electron-ion pairs to be generated are calculated using fractional ionization formula $1 - exp\left(W(s^{-1})dt\right)$ at every time step where $W(s^{-1})$ is calculated from equation (2).

The current study examines the role of dynamic ionization on the interaction of the laser pulse with plasma wakes. Although assuming pre-ionized plasma in the simulation shows proper non-linear wakes on axis of propagation and high frequency linear wakes off-axis but it fails to correctly model the modulation in the laser pulse and Raman scattering instabilities. This effect of ionization on modulation of the laser pulse and scattering of laser's electromagnetic waves with electron plasma waves can be attributed to an approximately linear increase in plasma density in the propagation direction of the laser pulse.

SIMULATION PARAMETERS

Simulation results reported here were performed using the parallel relativistic Particle-in-Cell code, SPACE, developed

at SBU and BNL. Minimum of 10 cells per wavelength in the propagation direction and a minimum of 20 cells per beam waist in polarization direction were used. Simulations use 32 macroparticles per cell. Numerical convergence studies confirmed that this resolution is sufficient for the study of targeted problems.

RESULTS AND DISCUSSIONS

First, we present results of the propagation of CO_2 laser in pre-ionized plasma with the density of 5.0×10^{17} cc^{-1}. Modulation of the on-axis laser electric field and corresponding spectrum are shown in Figures 1a and 1b, respectively. The spectrum shows a strong Stokes side band at $k_0 - k_p$, where k_0 and k_p are laser and plasma wavenumbers respectively. The corresponding amplitude of the anti-Stokes peak is much smaller.
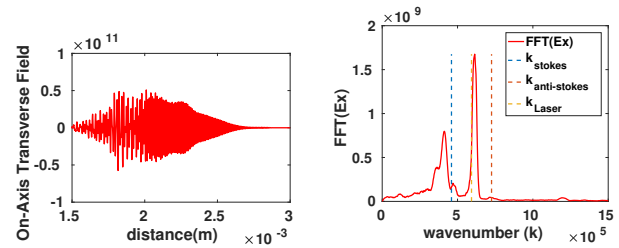
(a) on-axis laser field for propagation in pre-ionized plasma

(b) Spectrum of on-axis laser field for propagation in pre-ionized plasma

Figure 1: Self-modulation of laser field and corresponding spectrum

Next, we present the effects of including ionization model in the simulation. All numerical and physical parameters have been kept the same with only difference being the inclusion of ionization model. Figure 2 shows the charge density plot. Modulation of the on-axis laser electric field and the corresponding spectrum are shown in Figures 3a and 3b, respectively. The spectrum shows both Stokes and anti-Stokes side-bands of comparable amplitude at $k_0 - k_p$ and $k_0 + k_p$, respectively. Very strong modulation in the initial part of the laser pulse can be seen in this case. These effects can be attributed to an approximately linear increase in plasma density in the direction of propagation of the laser pulse as shown in figure.

Finally, we present the effects of laser beam quality on the intensity of Stokes/anti-Stokes peaks. Laser beam quality is quantified by the beam parameter product (BPP), which for a Gaussian beam is the product of the beam's divergence and waist size w_0. Laser beam quality factor M^2, which is defined as the ratio of the BPP of the real beam to that of an ideal Gaussian beam at the same wavelength is one for an ideal Gaussian beam but it increases as the beam quality worsens. Beams delivered by the laser systems used in experiments have M^2 value greater than one and are far from being ideal Gaussian, and therefore it is important to simulate non-Gaussian beams having higher M^2.
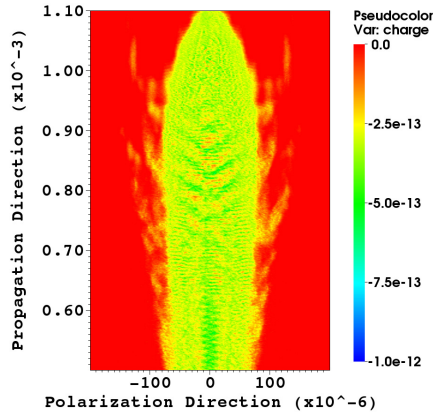
03 Novel Particle Sources and Acceleration Technologies

A22 Plasma Wakefield Acceleration

Figure 2: Charge density distribution showing formation of wakes

(a) on-axis laser field after propagating through H_2 gas

(b) Spectrum of on-axis laser field after propagating through H_2 gas
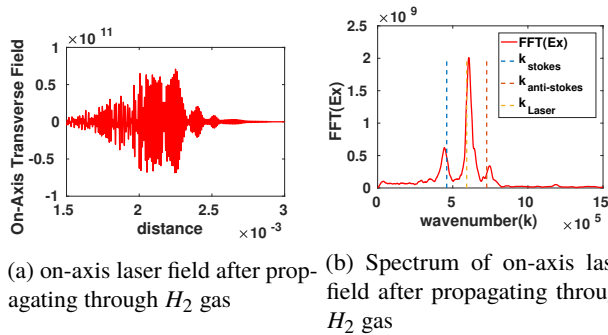
Figure 3: Self-modulation of laser field and corresponding spectrum

In order to calculate M^2 of the simulated beam, ISO standard procedure was followed [9]. Diameter of the laser beam was determined at several locations in the path of the beam using $D4\sigma$ method by calculating first and second order moments of the intensity distribution. The measured diameters were then fit to the hyperbolic function $\sqrt{a + bz + cz^2}$, where z is the location of diameter measurement and the fitting parameters a, b and c were determined using non-linear least square fitting algorithm. M^2 was then determined using the formula:

$$M^2 = \frac{\pi}{8\lambda}\sqrt{4ac - b^2}. \tag{3}$$

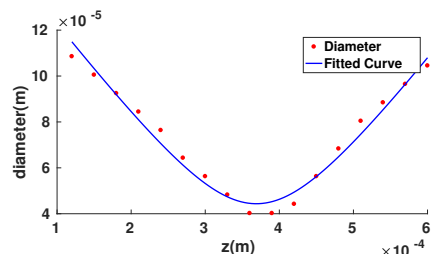Figure 4 shows one typical M^2 measurement procedure.

Figure 4: M^2 measurement of simulated beam

In the simulations presented above, the M^2 quality factor of the last beam was equal to 1.4. Now, we present two additional simulations which used the hydrogen gas ionization model and last beams with the quality factors M^2 of 2.08 and 2.8 respectively. Figure 5 shows the decrease in Stokes and anti-Stokes peaks with decreasing laser beam quality.
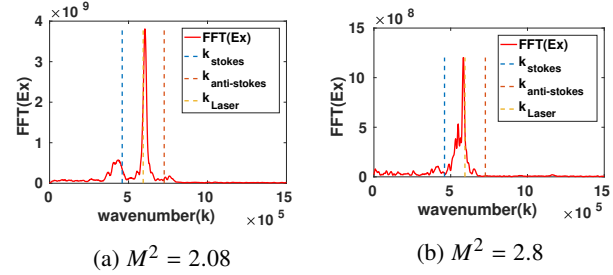

(a) $M^2 = 2.08$

(b) $M^2 = 2.8$

Figure 5: Effect of laser beam quality on EM spectra

CONCLUSION

3D numerical simulations of the interaction of a CO_2 laser with hydrogen jets have been presented. Simulations indicate that the self-modulation of the laser field and Raman scattering instabilities differ in the cases of pre-ionized plasma and the generation of plasma by the laser ionization of neutral hydrogen. In the case of pre-ionized plasma, a strong signal corresponding to Stokes frequency is present but the signal corresponding to the anti-Stokes frequency is very week. Simulation with the ionization model shows strong Stokes and anti-Stokes peaks which is attributed to the variation in plasma density in the propagation direction due to dynamic ionization. In addition, with the increase in the laser beam quality parameter (M^2), the intensity of the Stoke/anti-Stokes side bands decrease. In the presence of ionization, an increase of the plasma density along the laser path leads to the self-upshift of the laser frequency. Similar upshift of the laser frequency in the case of pre-ionized plasma is caused by the initially created gradient of the plasma density at the plasma edge.

ACKNOWLEDGMENTS

REFERENCES

[1] J.R. Welch et.al., "Mid-IR, CO_2-Laser driven, Self-Modulated Wakes" in Conference on Lasers and Electro-Optics, OSA Technical Digest (online) (Optical Society of America, 2017), paper FM2D.6.

[2] S.P.D. Mangles, "An Overview of Recent Progress in Laser-Wakefield Acceleration Experiments." `https://arxiv.org/pdf/1705.10588.pdf2017`

[3] W.D. Kimura, et.al., "Demonstration of High-Trapping Efficiency and Narrow Energy Spread in a Laser-Driven Accelerator," Phys. Rev. Lett. vol. 92, pp. 054801, 2004

[4] W.D. Kimura, et.al., "Laser Wakefield Acceleration Driven by a CO_2 Laser (STELLA-LW)-Final Report", (No. DOE/ER/41294-1 Final Report). STI Optronics, Inc., 2008.

[5] K. Yu, R. Samulyak, K. Yonehara and B. Freemire, "Simulation of beam-induced plasma in gas-filled RF cavities", Phys. Rev. Accel. Beams vol. 20, pp. 032002, 2017.

[6] E. Esarey, P. Sprangle, J. Krall, and A. Ting, "Overview of plasma-based accelerator concepts", IEEE Transactions on Plasma Science, vol. 24(2), pp.252-288, 1996.

[7] W. P. Leemans, C. W. Siders, E. Esarey, N. E. Andreev, G. Shvets, and W. B. Mori, "Plasma guiding and wakefield generation for second-generation experiments", IEEE Transactions on Plasma Science, vol. 24(2), pp. 331-342, 1996.

[8] D. L. Bruhwiler, D. A. Dimitrov, J. R. Cary, E. Esarey, W. Leemans, and R. E. Giacone, "Particle-in-cell simulations of tunneling ionization effects in plasma-based accelerators", Physics of Plasmas, vol. 10(5), pp.2022-2030, 2003.

[9] ISO/IEC 11146-1:2005 Lasers and laser-related equipment, "Test methods for laser beam widths, divergence angles and beam propagation ratios", Part 7: Beam widths and beam diameter measurement.